

Hierarchical Training of Deep Ensemble Policies for Reinforcement Learning in Continuous Spaces

Gang Chen¹ and Victoria Huang²

¹School of Engineering and Computer Science, Victoria University of Wellington, New Zealand

²National Institute of Water and Atmospheric Research, New Zealand

Abstract

Many actor-critic deep reinforcement learning (DRL) algorithms have achieved cutting-edge performance in tackling various challenging reinforcement learning (RL) problems, including complex control tasks with high-dimensional continuous state and action spaces. Despite of widely reported success, existing DRL algorithms often suffer from the ineffective exploration issue, resulting in limited learning stability and performance. To address this limitation, several ensemble DRL algorithms have been proposed recently to boost exploration and stabilize the learning process. However, many existing ensemble algorithms are designed to train each base learner individually without controlling explicitly the collaboration among the trained base learners. In this paper, we propose a new technique to train an ensemble of base learners based on the multi-step integration methods. The new multi-step training technique enables us to develop a new hierarchical training algorithm for ensemble DRL that promotes inter-learner collaboration through explicit inter-learner parameter sharing. The design of our new algorithm is verified theoretically. The algorithm is also shown empirically to outperform several cutting-edge DRL algorithms on multiple benchmark RL problems.

1 Introduction

Deep reinforcement learning (DRL) is a booming field of research in machine learning with diverse real-world applications [1]. In recent years, many *model-free* DRL algorithms achieved cutting-edge performance in tackling various continuous reinforcement learning (RL) problems, including complex control tasks with high-dimensional state and action spaces [2]. These algorithms can effectively train *deep neural networks* (DNNs) to precisely model high-quality control policies and are the central focus of this paper.

Despite of widely reported success, a majority of existing *actor-critic DRL algorithms*, such as DDPG [3], SAC [4] and PPO [5], still suffer from some major limitations. Specifically, existing research works showed that the algorithm performance is highly sensitive to hyper-parameter settings and can vary substantially in different algorithm runs [6]. *Ineffective exploration* is often considered as a major cause for the poor learning stability [7], often resulting in overfitting and premature convergence to poor local optima [8].

Rather than relying on one learner (or DRL agent), an ensemble of base learners can be jointly utilized to boost exploration and stabilize the learning process [9, 10]. For example, the *ensemble deep deterministic policy gradient* (ED2) algorithm is a newly developed ensemble DRL method [11] that trains multiple DNN policies simultaneously using a shared *experience replay buffer* (ERB), similar to several previously proposed parallel DRL algorithms [12, 13]. ED2 features a unique mixture of multiple well-studied tricks, including temporally-extended deep exploration, double Q-bias reduction, and target policy smoothing [9, 10, 14, 15]. It was reported to outperform state-of-the-art ensemble DRL algorithms such as SUNRISE [16] on several difficult Mujoco benchmark control problems.

As far as we know, most of the existing ensemble DRL algorithms are designed to train each base learner individually. For example, in ED2, every base learner trains its own DNN policy using its own critic, with the aim to improve its own performance without considering the impact of the trained policy on the ensemble. While sharing the same ERB, policy training is conducted largely independently by all base learners. This is shown to promote healthy exploration in [11]. However, there is no guarantee that the base learners will collaborate effectively such that the ensemble as a whole can achieve desirable performance.

To address this limitation, we propose a new *hierarchical approach* for training base learners in this paper. Specifically, we follow ED2 for *low-level training* of DNN policies, which will be performed concurrently by all base learners. In the meantime, we construct a *global critic*, which is trained constantly to predict the performance of the ensemble. Guided by the global critic, *high-level training* of DNN policies will be performed regularly to strengthen cooperation among all the base learners.

Since the ensemble is not used directly to collect state-transition samples from the learning environment, we must make sure that high-level training of the ensemble is not performed on *out-of-distribution* data obtained by individual base learners. In view of this, it is important to encourage *inter-learner parameter sharing* so that the DNN policy trained by one base learner can contribute directly to (or influence) the training of DNN policies by other base learners. For this purpose, we develop a new technique in this paper for high-level training of policies based on the *multi-step integration methods* for solving *ordinary differential equations* (ODEs) in [17].

Our high-level policy training technique is theoretically justified as it guarantees stability for a wide range of optimization problems. Meanwhile, it can be shown analytically that the trained linear parametric policies (a special and important technique for policy approximation) of all base learners are expected to behave more consistently as the ensemble through high-level policy training, encouraging inter-learner collaboration and alleviating the data distribution issue.

Driven by the hierarchical policy training method, we develop a new ensemble DRL

algorithm called *hierarchical ensemble deep deterministic policy gradient* (HED) in this paper. Experimental evaluation of HED has been conducted on a range of benchmark control problems, including the widely used Mujoco control tasks as well as the less popular and potentially more challenging PyBullet control problems. Our experiments clearly show that HED can outperform ED2, SUNRISE and several cutting-edge DRL algorithms on multiple benchmark problems.

2 Related Work

Similar to ED2, HED trains an ensemble of policies using an *off-policy* DRL algorithm to leverage on the algorithm’s advantages in *sample efficiency*. Recently, several off-policy DRL algorithms have been developed successfully for RL in continuous spaces, including DDPG [3], SAC [4], TD3 [15], and SOP [18]. These algorithms introduce a variety of tricks to stabilize the learning process. For example, TD3 extends the idea of double Q-network [14] to a new double-Q bias reduction technique, which can effectively prevent over-optimistic training of DNN policies. In addition, empirical evidence showed that the learning process becomes more stable when the actor and critic in TD3 are trained with different frequencies or in different phases [15, 19]. The base learners in our HED ensemble will adopt these tricks.

The recent literature also provides some new tricks to stabilize learning. Specifically, various trust-region methods have been developed to prevent negative behavioral changes during policy training [8, 20, 21, 22, 5]. Meanwhile, entropy regularization techniques prohibit immature convergence of the trained policies and ensure prolonged profitable exploration [23, 4]. However, these techniques are mainly applied to stochastic policies while we aim at learning an ensemble of deterministic policies. Previous research showed that deterministic policies can often be trained more efficiently than stochastic policies using the *reparameterization trick* [15, 24, 25].

The stability of a DRL algorithm depends critically on how the learner explores its environment. Besides the entropy regularization methods, curiosity metrics are popularly employed to encourage a learner to explore rarely visited states during RL [26, 27]. Meanwhile, many previous studies embraced the *optimum in the face of uncertainty* (OFU) principle to design bonus rewards for actions with high potentials, thereby promoting exploration in promising areas of the learning environment [28]. One good example is the UCB exploration technique developed in [29, 16]. However, in [11], this technique was shown to be less effective than the bootstrap with random initialization trick adopted in ED2. Temporally-extended exploration on RL problems with continuous actions can also be achieved by adding a small amount of noise to DNN weights [30]. This is directly related to the posterior sampling methods that are often used to select the best actions among a statistically plausible set of sampled actions [31].

Following the OFU principle, deep ensembles have been recently proposed to approximate Bayesian posteriors with high accuracy and efficiency [32]. They are subsequently used to approach deep exploration for reliable RL [9]. Several issues have been investigated under the context of ensemble DRL. For instance, the diversity of base learners is essential to the performance of the ensemble. To encourage diversity, either

different DRL algorithms or the same algorithm with differed hyper-parameter settings have been adopted to train base learners [33, 34]. Meanwhile, proper aggregation of the action outputs from all base learners in an ensemble poses another challenge. Typical approaches to tackle this issue include taking the mean action as the output of the ensemble and choosing the action with highest predicted cumulative rewards [11, 35].

As far as we know, few existing ensemble DRL algorithms in the literature have ever studied the important issue on how to effectively train all base learners to jointly improve the ensemble performance. This issue will be explored in-depth with the newly developed HED algorithm in this paper.

3 Background

An RL problem is modeled as a *Markov Decision Process* (MDP) $(\mathcal{S}, \mathcal{A}, R, P, \gamma, p_0)$, where \mathcal{S} and \mathcal{A} refer respectively to the continuous multi-dimensional state space and action space. P stands for the state-transition model that governs the probability of reaching any state $s_{t+1} \in \mathcal{S}$ at timestep $t + 1$ upon performing any action $a_t \in \mathcal{A}$ in state $s_t \in \mathcal{S}$ at timestep t , with $t \in \mathbb{Z}^+$. Additionally, $\gamma \in [0, 1)$ is the discount factor, R is the reward function, and p_0 captures the initial state distribution.

To solve any RL problem described above, we aim to learn an optimal *deterministic ensemble policy* $\pi_*^e(s)$ that maps any state input $s \in \mathcal{S}$ to an action vector $a \in \mathcal{A}$ so as to maximize the *cumulative rewards* defined below

$$\pi_*^e = \arg \max_{\pi^e} J(\pi^e) = \arg \max_{\pi^e} \mathbb{E}_{\tau \sim \pi^e} \left[\sum_{t=1}^{\infty} \gamma^{t-1} R(s_t, a_t) \right],$$

where $\tau = [(s_t, a_t, r_t, s_{t+1})]_{t=1}^{\infty}$ contains a series of consecutive state-transition samples and is called a *episode*, which can be obtained by following the ensemble policy π^e , and $r_t = R(s_t, a_t)$ is the immediate reward received at timestep t in τ . For an ensemble with N base learners where each base learner L_i , $1 \leq i \leq N$, maintains its own deterministic base policy π^i , the action output of π^e is jointly determined by all the *base policies* according to

$$\forall s \in \mathcal{S}, \pi^e(s) = \frac{1}{N} \sum_i^N \pi^i(s). \quad (1)$$

In order to train an ensemble to maximize the cumulative rewards, our baseline algorithm ED2 uses randomly selected base learners to sample a series of episodes $\{\tau_i\}$, which will be stored in the shared ERB. At regular time intervals, a mini-batch of state-transition samples will be retrieved from the ERB. Every base learner L_i will then use the retrieved mini-batch to train its own actor π^i and critic Q^i individually. In other words, a base learner manages two separate DNNs, one models the deterministic policy π^i and the other approximates the Q-function Q^i of π^i . A base learner uses an existing actor-critic RL algorithm to train the two DNNs. In this paper, we choose TD3 for this purpose due to its proven effectiveness, high popularity and stable learning behavior [15].

4 Hierarchical Ensemble Deep Deterministic Policy Gradient

The pseudo-code of the HED algorithm is presented in Algorithm 1. HED follows many existing works including ED2 [9, 11] to achieve temporally-extended exploration through bootstrapping with random initialization of DNN policies. As clearly shown in [11], this exploration technique is more effective than UCB and parameter randomization methods. Different from ED2 which completely eliminates the necessity of adding small random noises to the deterministic action outputs from the DNN policies, we keep a small level of action noise¹ while using any chosen policy to explore the learning environment. We found empirically that this ensures coherent exploration, similar to [9], while making the testing performance of the trained policies more stable.

Different from ED2 and other ensemble algorithms for RL in continuous spaces, HED trains DNN policies at two separate levels. The low-level training of π^i and Q^i by each base learner L_i is essentially the same as ED2 and TD3. Specifically, for any base learner $L_i, i \in \{1, \dots, N\}$, Q^i is trained by L_i to minimize MSE_i below

$$MSE_i = \frac{1}{|\mathcal{B}|} \sum_{(s,a,r,s') \in \mathcal{B}} \left(Q_{\phi_i}^i(s, a) - r - \gamma \min_{k=1,2} \hat{Q}_k^i(s', \pi^i(s') + \epsilon) \right)^2, \quad (2)$$

where ϕ_i represents the trainable parameters of the DNN that approximates Q^i . \mathcal{B} is the random mini-batch retrieved from the ERB. \hat{Q}_k^i with $k = 1, 2$ stands for the two target Q-networks of L_i that together implement the double-Q bias reduction mechanism proposed in [15]. Additionally, ϵ is a random noise sampled from a Normal distribution with zero mean and small variance². Using the trained Q^i , the trainable parameters θ_i of the DNN that models policy π^i is further updated by L_i along the *policy gradient* direction computed below

$$\nabla_{\theta_i} J(\pi_{\theta_i}^i) = \frac{1}{|\mathcal{B}|} \sum_{s \in \mathcal{B}} \nabla_a Q^i(s, a)|_{a=\pi_{\theta_i}^i(s)} \nabla_{\theta_i} \pi_{\theta_i}^i(s). \quad (3)$$

Besides the above, HED constantly trains a separate high-level Q-function Q^e to predict the performance of the ensemble policy π^e . Guided by the trained Q^e , high-level policy training is conducted regularly to update policy π^i of all base learners so as to enhance their cooperation and performance.

A new *multi-step technique* is developed in HED to enable inter-learner parameter sharing during high-level policy training. To implement this technique, we keep track of a list of bootstrap policy parameters for the multi-step training process. More details can be found in the subsequent subsection. Theoretical justifications regarding the usefulness of the multi-step approach are also provided below.

¹The noise is sampled from the Normal distribution independently for each dimension of the action vector. The variance of the normal distribution is fixed at 0.01 during the learning process.

²The variance for sampling ϵ is kept at a very small level of 0.01 in the experiments.

Algorithm 1 The pseudo-code of the HED algorithm.

Input: Ensemble size N ; initial policy networks $\pi_{\theta_i}^i$ and Q-networks $Q_{\phi_i}^i$ for $i \in \{1, \dots, N\}$; ERB; ensemble Q-network $Q_{\phi_e}^e$; target Q-networks for each base learner and the ensemble

Output: Trained ensemble policy π^e

While the total number of sampled trajectories $<$ max number of trajectories:
 Randomly sample $i \in \{1, \dots, N\}$
While the current trajectory does not terminate:
 Use π^i to perform the next action
 Store sampled state-transition in ERB
 Track number of steps sampled before critic training
If time for critic training:
 For number of steps sampled: q
 Sample a mini-batch \mathcal{B} from ERB
 Train $Q_{\phi_i}^i$ for $i \in \{1, \dots, N\}$ using (2)
 Train $Q_{\phi_e}^e$ using (4)
 If time for **low-level** policy training:
 Train $\pi_{\theta_i}^i$ for $i \in \{1, \dots, N\}$ using (3)
 If time for **high-level** policy training:
 Set bootstrap list $\{x_j\}_{j=0}^2$ for each base learner
 For a fraction of sampled steps:
 Train $\pi_{\theta_i}^i$ for $i \in \{1, \dots, N\}$ using (9)
 Append trained θ_i for $i \in \{1, \dots, N\}$ to the bootstrap lists of each base learner for the next step of high-level policy training

4.1 A multi-step technique for high-level policy training

In addition to Q^i for each base learner L_i , $i \in \{1, \dots, N\}$, HED maintains a separate Q-network to approximate Q^e of the ensemble policy π^e . Similar to (2), HED trains this central Q-network towards minimizing MSE_e below

$$MSE_e = \frac{1}{|\mathcal{B}|} \sum_{(s,a,r,s') \in \mathcal{B}} \left(Q_{\phi_e}^e(s,a) - r - \gamma \hat{Q}^e(s', \pi^e(s')) \right)^2, \quad (4)$$

with ϕ_e representing the trainable parameters of the central Q-network. \hat{Q}^e stands for the corresponding target Q-network that stabilizes the training process. For simplicity, we do not add random noise ϵ in (2) to the action outputs produced by the ensemble policy π^e in (4). Furthermore, following [14], one target Q-network instead of two is adopted in (4) to facilitate the training of Q^e . Building on the trained Q^e , we can calculate the *ensemble policy gradient* with respect to θ_i of every base learner L_i as follows

$$\nabla_{\theta_i} J(\pi^e) = \frac{1}{|\mathcal{B}|} \sum_{s \in \mathcal{B}} \nabla_a Q^e(s,a)|_{a=\pi^e(s)} \nabla_{a_i} \pi^e(s)|_{a_i=\pi_{\theta_i}^i(s)} \nabla_{\theta_i} \pi_{\theta_i}^i(s), \quad (5)$$

with

$$\nabla_{a_i} \pi^e(s)|_{a_i=\pi_{\theta_i^i}^i(s)} = \frac{1}{N} I,$$

according to (1). I stands for the $m \times m$ identity matrix where m is the dimension of the action vector. One straightforward approach for high-level policy training is to update θ_i of every base learner L_i in the direction of (5). However, using (5) alone may not encourage any base learner L_i to behave consistently with the ensemble (see Proposition 2). Consequently, high-level training of the ensemble policy may be performed on the out-of-distribution state-transition samples collected by the base learners, affecting the training effectiveness. Furthermore, ensembles are used mainly for temporally-extended exploration in the literature. The learning activity of one base learner can only influence other base learners indirectly through the shared ERB. Base learners do not explicitly share their learned policy parameters in an ensemble to strengthen inter-learner cooperation and boost the learning process.

To address this limitation, we propose to promote inter-learner parameter sharing during high-level policy training, in order to achieve a desirable balance between exploration and inter-learner cooperation. Specifically, in addition to (5), we randomly select *two base learners* L_p and L_q and use their policy parameters to guide the training of policy π^i of any base learner L_i . In comparison to *selecting one base learner*, this allows more base learners to have the opportunity to share their parameters with the base learner L_i during policy training. It is also possible to recruit more than two base learners. However, in this case, it is mathematically challenging to derive stable learning rules for high-level policy training.

Motivated by the above discussion, a search through the literature leads us to the linear multi-step integration methods recently analyzed in [17]. Consider a simple *gradient flow equation* below

$$x(0) = \theta_i^0, \frac{\partial x(t)}{\partial t} = g(x(t)) = \nabla_{\theta_i} J(\pi^e)|_{\theta_i=x(t)}, \quad (6)$$

where θ_i^0 refers to the initial policy parameter of base learner L_i . If $J(\pi^e)$ is strongly concave and Lipschitz continuous, the solution of (6) allows us to obtain the optimal policy parameters θ_i^* when $x(t)$ approaches to ∞ . Since $J(\pi^e)$ is not strongly concave for most of real-world RL problems, $x(t)$ in practice may only converge to a locally optimal policy, which is common among majority of the policy gradient DRL algorithms. Therefore high-level training of policy π^e and hence π^i can be approached by numerically solving (6). This can be achieved through a linear μ -step method shown below

$$x_{k+\mu} = - \sum_{j=0}^{\mu-1} \rho_j x_{k+j} + h \sum_{j=0}^{\mu-1} \sigma_j g(x_{k+j}), \forall k \geq 0, \quad (7)$$

where $\rho_j, \sigma_j \in \mathbb{R}$ are the pre-defined coefficients of the multi-step method and h is the learning rate. Clearly, each new point $x_{k+\mu}$ produced by the μ -step method is a function of the preceding μ points. In this paper, we specifically consider the case when $\mu = 3$. Meanwhile, let

$$x_0 = \theta_p, x_1 = \theta_q, x_2 = \theta_i \quad (8)$$

where p and q are the randomly generated indices of two base learners and i is the index of the base learner whose policy π^i is being trained by the μ -step method. Through this way, the training of policy π^i is influenced directly by base learners L_p and L_q through explicit inter-learner parameter sharing. $x_i (i \geq 3)$ in (7) represents the trained policy parameters of π^i in subsequent training steps.

Although (7) allows us to use $\nabla_{\theta_p} J(\pi^e)$ and $\nabla_{\theta_q} J(\pi^e)$ to train θ_i , they do not seem necessary for inter-learner parameter sharing. To simplify (7), we set $\sigma_0 = \sigma_1 = 0$ and $\sigma_2 = 1$. Hence only $g(x_{k+2})$, which is the ensemble policy gradient with respect to policy π^i in (5), is used to train π^i . With this simplification, we derive the new learning rule for high-level policy training below

$$\begin{aligned} x_{k+3} &= -\rho_2 x_{k+2} - \rho_1 x_{k+1} - \rho_0 x_k + h \cdot \nabla_{\theta_i} J(\pi^e)|_{\theta_i=x_{k+2}}, \forall k \geq 0 \\ x_0 &= \theta_p, x_1 = \theta_q, x_2 = \theta_i \end{aligned} \quad (9)$$

To implement (9) in HED, before high-level policy training, every base learner L_i must set up a *bootstrap list* of policy parameters $\{x_0 = \theta_p, x_1 = \theta_q, x_2 = \theta_i\}$. After the k -th training step ($k \geq 0$) based on (9), L_i appends the trained θ_i as x_{k+3} to the bootstrap list, which will be utilized to train π^i in the subsequent training steps. Reliable use of (9) demands for careful parameter settings of ρ_0, ρ_1, ρ_2 and h . Relevant theoretical analysis is presented below.

4.2 Theoretical analysis of the multi-step policy training technique

In this subsection, a theoretical analysis is performed first to determine suitable settings of ρ_0, ρ_1, ρ_2 and h for stable high-level policy training through (9). To make the analysis feasible, besides the strongly concave and Lipschitz continuous conditions, we further assume that

$$\nabla_{\theta_i} J(\pi^e) \approx -A(\theta_i - \theta_i^*) \quad (10)$$

where A is a positive definite matrix whose eigenvalues are bounded positive real numbers. θ_i^* stands for the global-optimal (or local-optimal) policy parameters. Many strongly concave functions satisfy this assumption [17]. Meanwhile, the attraction basin of the local optimum of many multi-modal optimization problems often satisfies this assumption too. Using this assumption, we can derive Proposition 1 below.

Proposition 1. *Upon using (9) to numerically solve (6), the following conditions must be satisfied for x_k to converge to θ_i^* as k approaches to ∞ :*

1. $\rho_2 = \rho_0 - 1, \rho_1 = -2\rho_0$;
2. $0 < \rho_0 < \frac{1}{2}$;
3. h is reasonably small such that $0 \leq \lambda h < 2 - 4\rho_0$, where λ can take any real value between the smallest and the largest eigenvalues of the positive definite matrix A in (10).

The proof of Proposition 1 can be found in Appendix A. Proposition 1 provides suitable parameter settings for (9) and justifies its stable use for high-level policy training. We next show that (9) is also expected to make base learners behave more consistently with the ensemble, without affecting the behavior of the trained ensemble, when ρ_0 is sufficiently small. Consider specifically that each base learner L_i trains a linear parametric policy of the form:

$$\pi^i(s) = \Phi(s)^T \cdot \theta_i \quad (11)$$

where $\Phi(s)$ represents the *state feature vector* with respect to any input state s . For simplicity, we study the special case of scalar actions. However, the analysis can be easily extended to high-dimensional action spaces. Meanwhile, we use $Sin()$ and $Mul()$ to represent respectively the action output of a policy trained for one iteration on the same state s by using either the single-step method or the multi-step method in (9). The single-step method can be considered as a special case of the multi-step method with $\rho_2 = -1$ and $\rho_0 = \rho_1 = 0$. Using these notations, Proposition 2 is presented below.

Proposition 2. *When each base learner L_i , $i \in \{1, \dots, N\}$, trains its linear parametric policy π^i with policy parameters θ_i on any state $s \in \mathcal{S}$ and when $0 < \rho_0 < \frac{1}{3}$,*

1. $Sin(\pi^e(s)) = \mathbb{E}[Mul(\pi^e(s))];$
2. $\sum_{i \in \{1, \dots, N\}} \mathbb{E} \left[(Mul(\pi^i(s)) - \mathbb{E}[Mul(\pi^e(s))])^2 \right]$
 $< \sum_{i \in \{1, \dots, N\}} (Sin(\pi^i(s)) - Sin(\pi^e(s)))^2$
 $= \sum_{i \in \{1, \dots, N\}} (\pi^i(s) - \pi^e(s))^2$

where the expectations above are taken with respect to any randomly selected $p, q \in \{1, \dots, N\}$ in (8).

Proposition 2 indicates that multi-step training in (9) is expected to reduce the difference between the action output of any base learner and that of the ensemble. Meanwhile the amount of action changes applied to π^e remains identical to the single-step method. Therefore, using the multi-step policy training method developed in this section helps to enhance consistent behaviors among all base learners of the ensemble.

Table 1: Final performance of all competing algorithms on 9 benchmark problems. The results are shown with mean cumulative rewards and standard deviation over 10 independent algorithm runs. For each run, the cumulative rewards are obtained by averaging over 50 independent testing episodes.

	TD3	SAC	ED2	SUNRISE	HED
Hopper-v0 (PyBullet)	917.38±178.46	1365.47±281.3	2095.54±148.86	1976.86±311.24	2359.63±50.28
InvertedDoublePendulum-v0 (PyBullet)	4394.07±558.8	8664.3±187.83	8733.3±1490.51	8746.82±58.68	9351.56±13.65
InvertedPendulum-v0 (PyBullet)	484.08±49.64	937.33±8.0	999.51±1.0	933.58±9.03	995.96±7.56
Reacher-v0 (PyBullet)	8.42±1.07	17.43±0.66	15.36±2.24	17.65±0.44	17.35±0.82
Hopper-v3 (Mujoco)	1399.54±250.32	2369.61±906.85	3043.19±971.53	2913.56±475.48	3503.08±83.35
Humanoid-v3 (Mujoco)	458.77±116.08	1720.54±525.07	868.17±384.58	3614.89±1402.7	3925.81±1029.59
LunarLanderContinuous-v2	254.98±17.86	254.03±27.52	268.37±6.9	278.76±2.34	278.23±3.51
Swimmer-v3 (Mujoco)	68.52±33.54	40.37±1.01	87.81±28.79	49.45±0.47	89.23±26.78
Walker2D-v3 (Mujoco)	1965.25±248.21	1503.35±818.87	3298.73±1282.64	3766.55±1063.0	4442.8±408.88

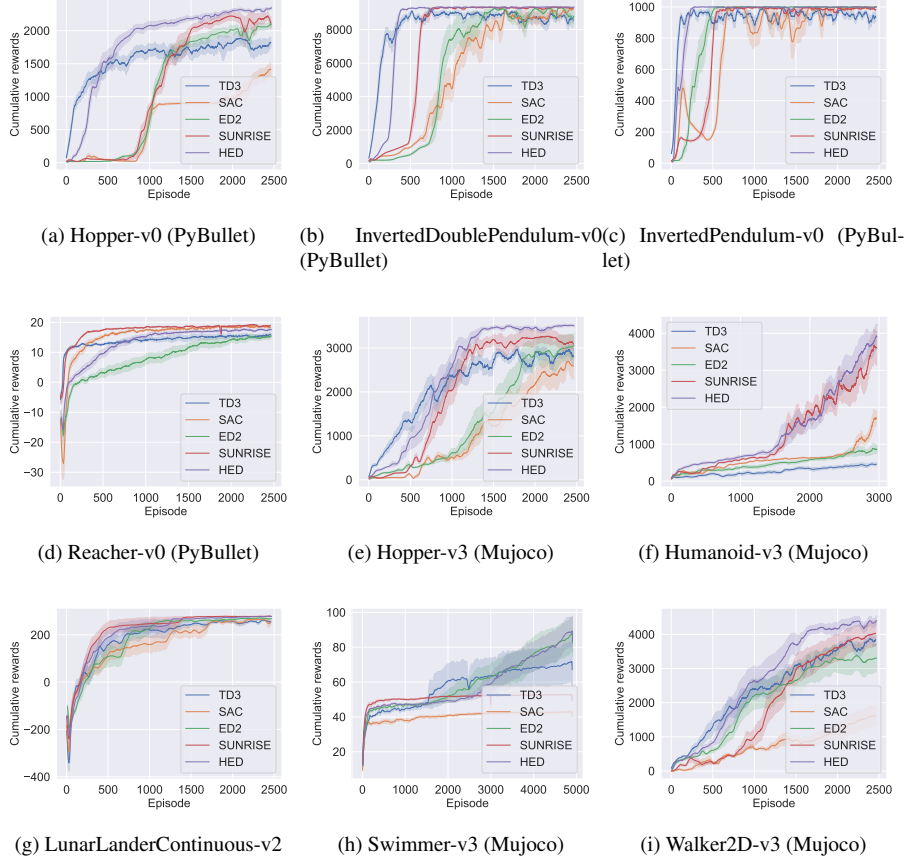


Figure 1: Learning curves of HED and four baseline algorithms (i.e., TD3, SAC, ED2 and SUNRISE) on 9 benchmark RL problems.

5 Experiment

This section presents the experimental evaluation of HED, in comparison to several state-of-the-art DRL algorithms. The experiment setup is discussed first. Detailed experiment results are further presented and analyzed.

5.1 Experiment setting

We implement HED based on the high-quality implementation of TD3 provided by the publicly available OpenAI Spinning Up repository [36]. We also follow closely the hyper-parameter settings of TD3 recommended in [15] to build each base learner of HED. Specifically, based on [5], a fully connected MLP with two hidden layers

of 64 ReLU units is adopted to model all policy networks and Q-networks. Similar to [11, 16], HED employs 5 base learners, i.e., $N = 5$. Each base learner has its own policy network and Q-network. Meanwhile, HED maintains and trains a separate ensemble Q-network with the same network architecture design.

Each base learner trains its Q-network and also conducts the low-level training of the policy network repeatedly whenever HED collects 50 consecutive state-transition samples from the learning environment. Meanwhile, high-level policy training as well as the training of the ensemble Q-network is performed immediately after HED samples a full episode. HED adopts a separate Adam optimizer with the fixed learning rate of $5e-4$ to train each Q-network and policy network. Furthermore, ρ_0 in (9) is set to 0.0001 for the main experiment results reported in Figure 1. The mini-batch size $|\mathcal{B}|$ is set to 100, following existing research [11] without any fine-tuning.

HED is compared against four state-of-the-art DRL algorithms, including two Ensemble DRL algorithms, i.e., ED2 [11] and SUNRISE [16]), and two widely used off-policy DRL algorithms, i.e., SAC [4] and TD3 [15]. We evaluate their performance on 9 challenging continuous control benchmark problems, including four PyBullet benchmark problems [37] (i.e., Hopper-v0, InvertedDoublePendulum-v0, InvertedPendulum-v0, and Reacher-v0), four Mujoco control tasks (i.e., Hopper-v3, Humanoid-v3, Swimmer-v3, and Walker2D-v3), and LunarLanderContinuous-v2 provided by OpenAI Gym [38]. In the literature, PyBullet benchmarks are often considered to be more challenging than Mujoco benchmarks. Hence we decide to evaluate the performance of HED on both PyBullet and Mujoco benchmarks. The maximum episode length for each benchmark is fixed to 1000 timesteps. Each algorithm is run independently with 10 random seeds on all benchmarks. Besides the hyper-parameter settings of HED highlighted above, detailed hyper-parameter settings of all the competing algorithms have been summarized in Appendix C.

5.2 Experiment result

5.2.1 Performance comparison:

We compare HED against four cutting-edge DRL algorithms on 9 benchmark problems. Table 1 presents the average cumulative rewards obtained by the policy networks (or policy ensembles for ensemble DRL algorithms) trained by all the competing algorithms across the same number of sampled episodes with respect to each benchmark. As evidenced in the table, HED achieved consistently the best performance³ on most of the benchmark problems except InvertedPendulum, Reacher, and LunarLander. Meanwhile, on InvertedPendulum, Reacher, and LunarLander, HED achieved very competitive performance with at least 98% of the maximum cumulative rewards reached by the highest performing competing algorithms. Furthermore, on some problems such as Hopper-v0 and Walker2D-v3, HED outperformed the lowest performing algorithm by up to 150% and the algorithm with the second highest performance by up to 18%.

In addition to Table 1, we also compared the learning curves of all the competing algorithms in Figure 1. As demonstrated in this figure, by explicitly strengthening inter-

³HED significantly outperformed ED2 on most benchmark problems, thanks to its use of the proposed high-level policy training technique.

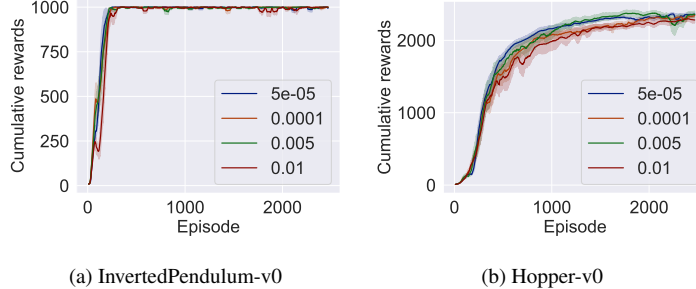


Figure 2: The impact of using different ρ_0 in (9) on the performance of HED. ρ_1 and ρ_2 in (9) depend directly on ρ_0 according to Proposition 1.

learner collaboration, HED converges clearly faster and is more stable during the learning process than other competing algorithms. Specifically, on several benchmark problems, such as Hopper-v0, InvertedDoublePendulum-v0, and Hopper-v3, HED achieved significantly lower variations in learning performance across 10 independent runs. In comparison to other ensemble DRL algorithms, the learning curves of HED also appear to be smoother on several benchmark problems, such as Walker2D-v3, suggesting that HED can achieve highly competitive stability during learning.

5.2.2 Impact of ρ_0 :

To investigate the performance impact of ρ_0 , we tested 4 different settings of ρ_0 , ranging from $5e-05$ to 0.01 , on the InvertedPendulum-v0 and Hopper-v0 problems (similar observations can be found on other benchmark problems and are omitted in this paper). The learning curves are plotted in Figure 2. It is witnessed in the figure that HED can convergence faster under suitable settings of ρ_0 . However, the “best” ρ_0 varies on different benchmark problems. For example, $\rho_0 = 0.005$ (green curve) converges slightly faster than other settings on InvertedPendulum-v0 while $\rho_0 = 5e-05$ (blue curve) converges slightly faster on Hopper-v0. Nevertheless, the impact of different ρ_0 on the final performance appears to be small as long as ρ_0 is reasonably small according to Proposition 1.

5.2.3 Ablation study on high-level policy training techniques:

High-level policy training can be conducted repeatedly whenever HED obtains either a new sampled episode or a fixed number of consecutive state-transition samples (e.g., samples collected from 50 consecutive timesteps). To understand which approach is more effective, experimental comparisons have been conducted in Appendix D with detailed performance results. According to the experiment results in Appendix D, on a majority of benchmark problems, episodic learning can produce more stable learning behavior and also makes HED converge faster.

We also compared HED with its variation that performs high-level policy training by using the single-step method in (5) instead of the multi-step method in (9). Detailed experiment results can be found in Appendix E. Our experiment results confirm that multi-step training in (9) enables HED to achieve significantly higher performance and learning stability than using the conventional single-step training technique in (5). Hence, by explicitly sharing learned policy parameters among base learners in an ensemble through (9), HED can effectively enhance inter-learner collaboration and boost the learning process.

6 Conclusions

In this paper, we conducted in-depth study of ensemble DRL algorithms, which have achieved cutting-edge performance on many benchmark RL problems in the recent literature. Different from existing research works that rely mainly on each base learner of an ensemble to train its policy network individually, we developed a new HED algorithm to explore the potential of training all base learners in a hierarchical manner in order to promote inter-learner collaboration and improve the collective performance of an ensemble of trained base learners. Specifically, we adopted existing ensemble DRL algorithms such as ED2 to perform low-level policy training. Meanwhile, a new multi-step training technique was developed for high-level policy training in HED to facilitate direct inter-learner parameter sharing. Both theoretical and empirical analysis showed that the HED algorithm can achieve stable learning behavior. It also outperformed several state-of-the-art DRL algorithms on multiple benchmark RL problems.

Appendix A

This appendix presents a proof of Proposition 1. According to [17], any multi-step integration methods including (9) must satisfy three conditions to ensure its stability. They together guarantee that x_k can converge to θ_i^* as k approaches to ∞ . We check each condition one-by-one below to derive the main conclusions in Proposition 1.

Consistency condition: We can re-write (9) as below

$$x_{k+3} + \rho_2 x_{k+2} + \rho_1 x_{k+1} + \rho_0 x_k = h \cdot g(x_{k+2}).$$

Define the *shift operator* F , which maps $Fx_k \rightarrow x_{k+1}$. Furthermore, with $g(x_k)$ being simplified to g_k , F also maps $Fg_k \rightarrow g_{k+1}$. Using F , (9) can be further written as

$$\rho(F)x_k = h\sigma(F)g_k, \forall k \geq 0,$$

where

$$\rho(F) = F^3 + \rho_2 F^2 + \rho_1 F + \rho_0, \sigma(F) = F^2.$$

The consistency condition requires

$$\rho(1) = 0, \rho'(1) = \sigma(1).$$

This implies that

$$\begin{aligned} 1 + \rho_2 + \rho_1 + \rho_0 &= 0, \\ 3 + 2\rho_2 + \rho_1 &= 1. \end{aligned}$$

Solving the above equations leads to

$$\rho_1 = -2\rho_0, \rho_2 = \rho_0 - 1.$$

Hence, (9) becomes

$$x_{k+3} = (1 - \rho_0)x_{k+2} + 2\rho_0x_{k+1} - \rho_0x_k + h \cdot g(x_{k+2}).$$

Zero-stability condition: This condition requires all roots of $\rho(F)$ to be in the unit disk. Any roots on the unit circle must be simple. In other words,

$$|Roots(\rho(F))| \leq 1.$$

In fact, $\rho(F)$ has three roots. They are

$$1, \frac{1}{2} \left(-\rho_0 \pm \sqrt{\rho_0(\rho_0 + 4)} \right).$$

It is easy to verify that when $0 < \rho_0 < \frac{1}{2}$,

$$\left| \frac{1}{2} \left(-\rho_0 - \sqrt{\rho_0(\rho_0 + 4)} \right) \right| < 1.$$

Meanwhile, when $\rho_0 > 0$,

$$\left| \frac{1}{2} \left(-\rho_0 + \sqrt{\rho_0(\rho_0 + 4)} \right) \right| < 1.$$

In summary, the zero-stability condition requires

$$0 < \rho_0 < \frac{1}{2}.$$

Absolute stability condition: Define

$$\begin{aligned} \Pi_{\lambda h} &\triangleq \rho(F) + \lambda h \sigma(F) \\ &= F^3 + \rho_2 F^2 + \rho_1 F + \rho_0 + \lambda h F^2 \\ &= F^3 + (\rho_0 - 1) F^2 - 2\rho_0 F + \rho_0 + \lambda h F^2 \\ &= F^3 + (\rho_0 - 1 + \lambda h) F^2 - 2\rho_0 F + \rho_0. \end{aligned}$$

Further define

$$r_{max} = \max_{\lambda \in [L, U]} \max_{r \in Roots(\Pi_{\lambda h}(F))} |r|,$$

where L and U in this appendix refer respectively to the smallest and the largest positive eigenvalues of matrix A in (10). The absolute stability condition requires

$$r_{max} < 1. \quad (12)$$

Let

$$\begin{aligned} B &= \rho_0 - 1 + \lambda h, \\ C &= -2\rho_0, \\ D &= \rho_0. \end{aligned}$$

Subsequently, define

$$\begin{aligned} A_0 &= 1 - B + C - D = 2 - \lambda h - 4\rho_0, \\ A_1 &= 3 - B - C - 3D = 4 - \lambda h - 2\rho_0, \\ A_2 &= 3 + B - C - 3D = 2 + \lambda h, \\ A_3 &= 1 + B + C + D = \lambda h. \end{aligned}$$

According to the Routh-Hurwitz criterion [39], the following two conditions jointly guarantee (12):

$$\begin{aligned} A_1, A_2, A_3, A_4 &> 0, \\ A_1 A_2 &> A_0 A_3. \end{aligned}$$

Specifically, the first condition above gives rise to the following:

$$\lambda h > 0, \lambda h + 2\rho_0 < 4, \lambda h + 4\rho_0 < 2.$$

Following the second condition above, we can deduce the below:

$$\lambda h > 2 - \frac{4}{\rho_0}.$$

Given that $\lambda h > 0$, we have

$$\begin{aligned} \lambda h &> \max \left\{ 0, 2 - \frac{4}{\rho_0} \right\}, \\ \lambda h &< \min \{ 2 - 4\rho_0, 4 - 2\rho_0 \}. \end{aligned}$$

Since $0 < \rho_0 < \frac{1}{2}$,

$$2 - 4\rho_0 < 4 - 2\rho_0, \quad 2 - \frac{4}{\rho_0} < 0.$$

Consequently

$$0 < \lambda h < 2 - 4\rho_0.$$

Clearly, with sufficiently small h , the above condition on absolute stability can be easily satisfied. Hence, we can use (9) to perform high-level policy training stably in the HED algorithm.

Appendix B

This appendix presents a proof of Proposition 2. Considering any specific state $s \in \mathcal{S}$, let

$$\nabla_a Q^e(s, a)|_{a=\pi^e(s)} = C,$$

where C is an arbitrary scalar constant, in line with the assumption of scalar actions. Using (1) and (11), the ensemble policy gradient with respect to policy parameters θ_i of policy π^i , $i \in [1, \dots, N]$, is

$$\nabla_{\theta_i} J(\pi^e) = \frac{C\Phi(s)}{N}.$$

According to the multi-step learning rule in (9), updating θ_i for one iteration gives the updated θ_i as

$$(1 - \rho_0)\theta_i + 2\rho_0\theta_q - \rho_0\theta_p + h\frac{C\Phi(s)}{N}.$$

Therefore,

$$Mul(\pi^i(s)) = (1 - \rho_0)\pi^i(s) + 2\rho_0\pi^q(s) - \rho_0\pi^p(s) + \frac{hC}{N}\Phi(s)^T\Phi(s).$$

Hence

$$\mathbb{E}[Mul(\pi^i(s))] = (1 - \rho_0)\pi^i(s) + \rho_0\pi^e(s) + \frac{hC}{N}\Phi(s)^T\Phi(s),$$

$$\mathbb{E}[Mul(\pi^e(s))] = \pi^e(s) + \frac{hC}{N}\Phi(s)^T\Phi(s).$$

In comparison, upon using the single-step method, the updated θ_i becomes

$$\theta_i + h\frac{C\Phi(s)}{N}.$$

Subsequently,

$$Sin(\pi^i(s)) = \pi^i(s) + \frac{hC}{N}\Phi(s)^T\Phi(s),$$

$$Sin(\pi^e(s)) = \pi^e(s) + \frac{hC}{N}\Phi(s)^T\Phi(s).$$

Clearly,

$$Sin(\pi^e(s)) = \mathbb{E}[Mul(\pi^e(s))].$$

Hence, the expected action changes applied to $\pi^e(s)$ are identical, regardless of whether single-step or multi-step method is used for high-level policy training⁴.

Define

$$\Delta = \sum_{i \in [1, \dots, N]} (\pi^i(s) - \pi^e(s)).$$

⁴We assume in Proposition 2 that high-level policy training is performed for one iteration on a specific state s .

For the single-step method, after all base learners trained their respective policies for one iteration on state s , it is easy to verify that

$$\begin{aligned}
& \sum_{i \in [1, \dots, N]} (\text{Sin}(\pi^i(s)) - \text{Sin}(\pi^e(s)))^2 \\
&= \sum_{i \in [1, \dots, N]} (\pi^i(s) - \pi^e(s))^2 \\
&= \Delta.
\end{aligned}$$

Meanwhile,

$$\begin{aligned}
& (\text{Mul}(\pi^i(s)) - \mathbb{E}[\text{Mul}(\pi^e(s))])^2 \\
&= ((1 - \rho_0)(\pi^i(s) - \pi^e(s)) + 2\rho_0(\pi^q(s) - \pi^e(s)) - \rho_0(\pi^p(s) - \pi^e(s)))^2 \\
&= (1 - \rho_0)^2(\pi^i(s) - \pi^e(s))^2 + 4\rho_0^2(\pi^q(s) - \pi^e(s))^2 + \rho^2(\pi^p(s) - \pi^e(s))^2 \\
&\quad + 4(1 - \rho_0)\rho_0(\pi^i(s) - \pi^e(s))(\pi^q(s) - \pi^e(s)) \\
&\quad - 2(1 - \rho_0)\rho_0(\pi^i(s) - \pi^e(s))(\pi^p(s) - \pi^e(s)) \\
&\quad - 4\rho_0^2(\pi^q(s) - \pi^e(s))(\pi^p(s) - \pi^e(s)).
\end{aligned}$$

Since the base learner indices p and q are randomly and independently selected,

$$\begin{aligned}
\mathbb{E}[(\pi^i(s) - \pi^e(s))(\pi^p(s) - \pi^e(s))] &= 0, \\
\mathbb{E}[(\pi^i(s) - \pi^e(s))(\pi^q(s) - \pi^e(s))] &= 0, \\
\mathbb{E}[(\pi^q(s) - \pi^e(s))(\pi^p(s) - \pi^e(s))] &= 0.
\end{aligned}$$

Therefore

$$\begin{aligned}
& \sum_{i \in [1, \dots, N]} \mathbb{E}[(\text{Mul}(\pi^i(s)) - \mathbb{E}[\text{Mul}(\pi^e(s))])^2] \\
&= (1 - \rho_0)^2\Delta + 4\rho_0^2\Delta + \rho_0^2\Delta \\
&= (1 - 2\rho_0 + 6\rho_0^2)\Delta.
\end{aligned}$$

When $0 < \rho_0 < \frac{1}{3}$,

$$1 - 2\rho_0 + 6\rho_0^2 < 1.$$

As a result,

$$\begin{aligned}
& \sum_{i \in [1, \dots, N]} \mathbb{E}[(\text{Mul}(\pi^i(s)) - \mathbb{E}[\text{Mul}(\pi^e(s))])^2] \\
&< \sum_{i \in [1, \dots, N]} (\text{Sin}(\pi^i(s)) - \text{Sin}(\pi^e(s)))^2.
\end{aligned}$$

Table 2: Hyper-parameter settings of competing algorithms.

Hyper-parameter	TD3	SAC	ED2	SUNRISE
Num. episodes	2500	2500	2500	3000
Episode length	1000	1000	1000	1000
Minibatch size	100	100	100	256
Adam learning rate	5e-4	3e-4	5e-4	3e-4
Discount (γ)	0.99	0.99	0.99	0.99
GAE parameter (λ)	0.995	0.995	0.995	0.995
Replay buffer size	1e6	1e6	1e6	1e6
Update interval	50	50	50	50
Ensemble size	-	-	5	5

Appendix C

Table 2 provides detailed hyper-parameter settings of all competing algorithms. Our hyper-parameter settings follow strictly the recommended settings in [15, 4, 11, 16].

All experiments were run using a cluster of Linux computing nodes. Each node is equipped with 16 GB memory. The CPU specification is provided in Table 3. Each experiment was run in a Python virtual environment managed by Anaconda with Python packages specified in Table 4.

Table 3: CPU specification.

Architecture	x86_64
CPU op-mode(s)	32-bit, 64-bit
CPU(s)	16
CPU family	6
Thread(s) per core	2
CPU max MHz	4900.0000
CPU min MHz	800.0000
Model name	11th Gen Intel(R) Core(TM) i7-11700 @ 2.50GHz

Appendix D

In this appendix, we study the effectiveness of conducting high-level policy training after HED obtains a full sampled episode. Figure 3 shows the performance comparison of HED with two different training frequencies: every 50 consecutive timesteps vs. every episode. It can be noticed that, on a majority benchmark problems (i.e., 5 out of 6), performing high-level policy training after every episode (orange curve) can significantly improve the HED algorithm in terms of both the final performance and convergence speed. For example, as shown in Figure 3(e), the orange curve reaches 3500 after 1500 episodes while the blue curve converges to a lower cumulative reward (approx. 3000) after 2000 episodes.

Table 4: Python packages.

Package name	Version
cython	0.29.25
gym	0.21.0
keras	2.7.0
mujoco-py	2.1.2.14
numpy	1.21.4
pybulletgym	0.1
python	3.7.11
scipy	1.7.3
tensorflow	2.7.0

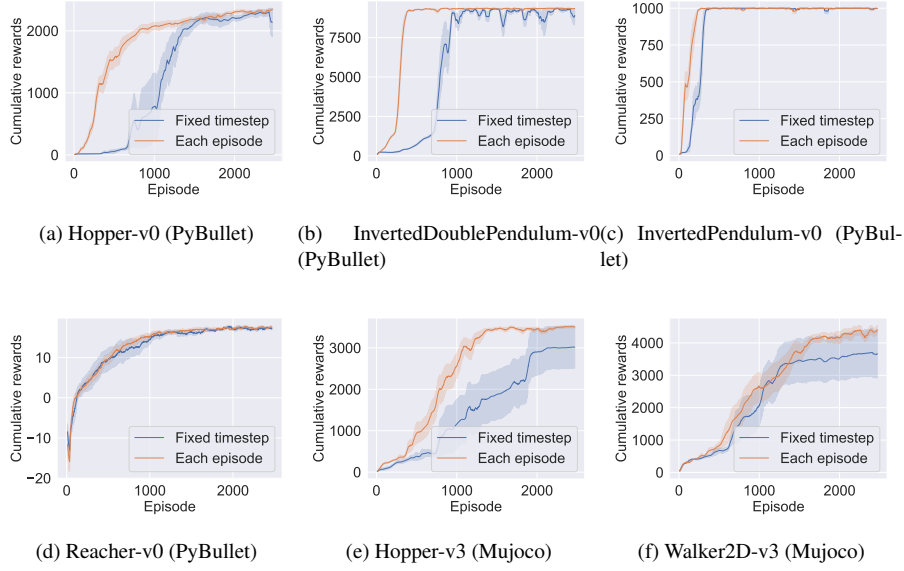


Figure 3: Learning curves of HED with respect to two high-level policy training approaches. The method that conducts high-level policy training after every 50 timesteps is denoted as *Fixed timestep*. The method that conducts high-level policy training at the end of each sampled episode is denoted as *Each episode*.

We also notice that episodic policy training is more robust to the randomness in the environment and less sensitive to the initialization of neural network weights. For example, in Figure 3(e), episodic policy training produces a smaller confident interval (orange shaded area) compared to the fixed timestep training (blue shaded area) over 10 independent algorithm runs. Similar results can also be observed from Figures 3(a) and (f). Note that in each algorithm run, both policy networks and Q-networks are initialized with different weights. The environment initial states also vary.

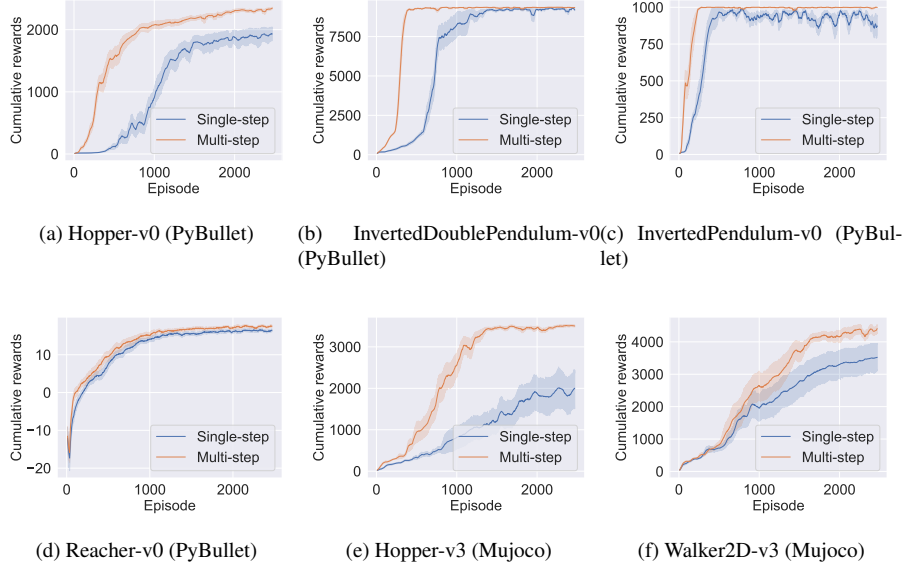


Figure 4: Learning curves of HED using the single-step high-level policy training technique in (5) vs. the proposed multi-step high-level policy training technique in (9).

Appendix E

This appendix investigates the effectiveness of multi-step policy training by using (9). Specifically, we compare the performance of HED against its variant, which performs single-step high-level policy training by using (5), on 6 problems that include both PyBullet and Mujoco benchmarks.

As shown in Figure 4, with the help of (9), significant performance improvement can be observed (orange curve) on most benchmark problems. In particular, HED behaves more stably during the learning process. For example, in Figure 4(c), the cumulative rewards obtained by the policy trained using (9) (orange curve) remain stable at 1000 after 300 episodes. In comparison, the blue curve stays below 1000 and fluctuates between 800 and 1000 over the entire learning period. Similar trends can also be noticed in Figure 4(b).

The proposed multi-step policy training technique achieves clearly higher cumulative rewards. In the Hopper environment shown in Figure 4(e), the orange curve outperforms the blue curve by up to 75% after 2500 training episodes. Moreover, the orange curve converges to 3500 while the blue curve remains below 2000. The significant improvement in cumulative rewards can also be witnessed in Figure 4(a) and (f).

The shaded areas in Figure 4(e) and (f) also show that the multi-step training technique is less sensitive to the environment randomness and neural network weight

initialization, compared to using the conventional single-step training method in (5). Hence, our experiment results confirm the importance of inter-learner collaboration. By enabling base learners in an ensemble to explicitly share their learned policy parameters, HED can achieve high learning stability and effectively boost the learning process.

References

- [1] J. Ibarz, J. Tan, C. Finn, M. Kalakrishnan, P. Pastor, and S. Levine, “How to train your robot with deep reinforcement learning: lessons we have learned,” *The International Journal of Robotics Research*, vol. 40, no. 4-5, pp. 698–721, 2021.
- [2] R. Liu, F. Nageotte, P. Zanne, M. de Mathelin, and B. Dresp-Langley, “Deep reinforcement learning for the control of robotic manipulation: a focussed mini-review,” *Robotics*, vol. 10, no. 1, p. 22, 2021.
- [3] T. P. Lillicrap, J. J. Hunt, A. Pritzel, N. Heess, T. Erez, Y. Tassa, D. Silver, and D. Wierstra, “Continuous control with deep reinforcement learning,” *arXiv preprint arXiv:1509.02971*, 2015.
- [4] T. Haarnoja, A. Zhou, P. Abbeel, and S. Levine, “Soft actor-critic: Off-policy maximum entropy deep reinforcement learning with a stochastic actor,” in *International conference on machine learning*. PMLR, 2018, pp. 1861–1870.
- [5] J. Schulman, F. Wolski, P. Dhariwal, A. Radford, and O. Klimov, “Proximal policy optimization algorithms,” *arXiv preprint arXiv:1707.06347*, 2017.
- [6] T. L. Paine, C. Paduraru, A. Michi, C. Gulcehre, K. Zolna, A. Novikov, Z. Wang, and N. de Freitas, “Hyperparameter selection for offline reinforcement learning,” *arXiv preprint arXiv:2007.09055*, 2020.
- [7] C. Y. S. Chan, S. Fishman, J. Canny, A. Korattikara, and S. Guadarrama, “Measuring the reliability of reinforcement learning algorithms,” *arXiv preprint arXiv:1912.05663*, 2019.
- [8] T. Kurutach, I. Clavera, Y. Duan, A. Tamar, and P. Abbeel, “Model-ensemble trust-region policy optimization,” *arXiv preprint arXiv:1802.10592*, 2018.
- [9] I. Osband, C. Blundell, A. Pritzel, and B. V. Roy, “Deep exploration via bootstrapped dqn,” *Advances in neural information processing systems*, vol. 29, pp. 4026–4034, 2016.
- [10] I. Osband and B. V. Roy, “Why is posterior sampling better than optimism for reinforcement learning?” in *International conference on machine learning*. PMLR, 2017, pp. 2701–2710.
- [11] P. Januszewski, M. Olko, M. Królikowski, J. Świątkowski, M. Andrychowicz, L. Kuciński, and P. Miloś, “Continuous control with ensemble deep deterministic policy gradients,” *arXiv preprint arXiv:2111.15382*, 2021.

- [12] G. Barth-Maron, M. W. Hoffman, D. Budden, W. Dabney, D. Horgan, D. Tb, A. Muldal, N. Heess, and T. Lillicrap, “Distributed distributional deterministic policy gradients,” *arXiv preprint arXiv:1804.08617*, 2018.
- [13] V. Mnih, A. P. Badia, M. Mirza, A. Graves, T. Lillicrap, T. Harley, D. Silver, and K. Kavukcuoglu, “Asynchronous methods for deep reinforcement learning,” in *International conference on machine learning*. PMLR, 2016, pp. 1928–1937.
- [14] H. V. Hasselt, A. Guez, and D. Silver, “Deep reinforcement learning with double q-learning,” in *Proceedings of the AAAI conference on artificial intelligence*, vol. 30, no. 1, 2016.
- [15] S. Fujimoto, H. Hoof, and D. Meger, “Addressing function approximation error in actor-critic methods,” in *International Conference on Machine Learning*. PMLR, 2018, pp. 1587–1596.
- [16] K. Lee, M. Laskin, A. Srinivas, and P. Abbeel, “Sunrise: A simple unified framework for ensemble learning in deep reinforcement learning,” in *International Conference on Machine Learning*. PMLR, 2021, pp. 6131–6141.
- [17] D. Scieur, V. Roulet, F. Bach, and A. d’Aspremont, “Integration methods and accelerated optimization algorithms,” *arXiv preprint arXiv:1702.06751*, 2017.
- [18] C. Wang, Y. Wu, Q. Vuong, and K. Ross, “Striving for simplicity and performance in off-policy drl: Output normalization and non-uniform sampling,” in *International Conference on Machine Learning*. PMLR, 2020, pp. 10 070–10 080.
- [19] K. W. Cobbe, J. Hilton, O. Klimov, and J. Schulman, “Phasic policy gradient,” in *International Conference on Machine Learning*. PMLR, 2021, pp. 2020–2027.
- [20] J. Schulman, N. Heess, T. Weber, and P. Abbeel, “Gradient estimation using stochastic computation graphs,” *Advances in Neural Information Processing Systems*, vol. 28, pp. 3528–3536, 2015.
- [21] L. Shani, Y. Efroni, and S. Mannor, “Adaptive trust region policy optimization: Global convergence and faster rates for regularized mdps,” in *Proceedings of the AAAI Conference on Artificial Intelligence*, vol. 34, no. 04, 2020, pp. 5668–5675.
- [22] Y. Wu, E. Mansimov, R. B. Grosse, S. Liao, and J. Ba, “Scalable trust-region method for deep reinforcement learning using kronecker-factored approximation,” *Advances in neural information processing systems*, vol. 30, pp. 5279–5288, 2017.
- [23] G. Chen, Y. Peng, and M. Zhang, “Effective exploration for deep reinforcement learning via bootstrapped q-ensembles under tsallis entropy regularization,” *arXiv preprint arXiv:1809.00403*, 2018.
- [24] D. Silver, G. Lever, N. Heess, T. Degris, D. Wierstra, and M. Riedmiller, “Deterministic policy gradient algorithms,” in *International conference on machine learning*. PMLR, 2014, pp. 387–395.

- [25] J. Baek, H. Jun, J. Park, H. Lee, and S. Han, “Sparse variational deterministic policy gradient for continuous real time control,” *IEEE Transactions on Industrial Electronics*, 2020.
- [26] P. Reizinger and M. Szemenyei, “Attention-based curiosity-driven exploration in deep reinforcement learning,” in *ICASSP 2020-2020 IEEE International Conference on Acoustics, Speech and Signal Processing (ICASSP)*. IEEE, 2020, pp. 3542–3546.
- [27] O. Zhelo, J. Zhang, L. Tai, M. Liu, and W. Burgard, “Curiosity-driven exploration for mapless navigation with deep reinforcement learning,” *arXiv preprint arXiv:1804.00456*, 2018.
- [28] M. Bellemare, S. Srinivasan, G. Ostrovski, T. Schaul, D. Saxton, and R. Munos, “Unifying count-based exploration and intrinsic motivation,” *Advances in neural information processing systems*, vol. 29, pp. 1471–1479, 2016.
- [29] R. Y. Chen, S. Sidor, P. Abbeel, and J. Schulman, “Ucb exploration via q-ensembles,” *arXiv preprint arXiv:1706.01502*, 2017.
- [30] M. Plappert, R. Houthoofd, P. Dhariwal, S. Sidor, R. Y. Chen, X. Chen, T. Asfour, P. Abbeel, and M. Andrychowicz, “Parameter space noise for exploration,” *arXiv preprint arXiv:1706.01905*, 2017.
- [31] I. Osband, J. Aslanides, and A. Cassirer, “Randomized prior functions for deep reinforcement learning,” *arXiv preprint arXiv:1806.03335*, 2018.
- [32] B. Lakshminarayanan, A. Pritzel, and C. Blundell, “Simple and scalable predictive uncertainty estimation using deep ensembles,” *arXiv preprint arXiv:1612.01474*, 2016.
- [33] Z. Huang, S. Zhou, B. Zhuang, and X. Zhou, “Learning to run with actor-critic ensemble,” *arXiv preprint arXiv:1712.08987*, 2017.
- [34] M. A. Wiering and H. V. Hasselt, “Ensemble algorithms in reinforcement learning,” *IEEE Transactions on Systems, Man, and Cybernetics, Part B (Cybernetics)*, vol. 38, no. 4, pp. 930–936, 2008.
- [35] G. Chen and Y. Peng, “Off-policy actor-critic in an ensemble: Achieving maximum general entropy and effective environment exploration in deep reinforcement learning,” *arXiv preprint arXiv:1902.05551*, 2019.
- [36] J. Achiam, “Spinning Up in Deep Reinforcement Learning,” <https://github.com/openai/spinningup>, 2018.
- [37] B. Ellenberger, “Pybullet gymperium,” <https://github.com/benelot/pybullet-gym>, 2018–2019.
- [38] G. Brockman, V. Cheung, L. Pettersson, J. Schneider, J. Schulman, J. Tang, and W. Zaremba, “Openai gym,” *arXiv:1606.01540*, 2016.
- [39] N. S. Nise, *Control systems engineering*. John Wiley & Sons, 2020.